中国激光

飞秒激光五轴扫描加工深盲孔

乔亚庆[1]，唐爱国[1]，陈天庭[1]，马浩然[1]，刘翌[1]，高辉[1,2]，熊伟[1,2]，邓磊敏[1,2*]

[1]华中科技大学武汉光电国家研究中心，湖北 武汉 430074；

[2]湖北光谷实验室，湖北 武汉 430074

摘要 采用五轴激光扫描技术研究了FR4覆铜板的深盲孔制造技术。通过实验研究了激光参数和扫描图形的填充间距对盲孔侧壁锥度和底部材料去除均匀性的影响，通过调节激光扫描策略，实现了盲孔锥度和孔径的连续调节。盲孔深度为925 μm，最大深径比可达4.9∶1，孔侧壁平直，孔底玻璃纤维复合材料被完全去除，铜层的损伤深度小于1 μm。实验结果表明，五轴激光扫描技术可以有效提升激光的盲孔制造能力。

关键词 激光技术；激光钻盲孔；五轴激光扫描；侧壁锥度；飞秒激光

中图分类号 TN41 **文献标志码** A **DOI**：10.3788/CJL230762

1 引 言

在FR4覆铜板上加工盲孔进而实现电子元器件互联是印刷电路板等领域的重要方法，盲孔制造质量是决定器件性能的关键一环[1-3]。激光加工具有精度高、无机械作用力和控制灵活等优势，是FR4覆铜板盲孔加工的主要方法[4-5]。由于树脂对波长为9.3～10.6 μm的CO_2激光有较高的吸收率，而铜对其吸收率很低，故CO_2激光被广泛应用于FR4覆铜板的盲孔制造[6-7]。CO_2激光脉冲加工具有极高的加工效率，但是只适用于孔径和孔深约为100 μm的微孔，并且CO_2激光的热效应严重，成孔精度难以保证[8-9]。纳秒紫外(UV)激光具有较高的光子能量，通过破坏材料的分子键来实现材料去除，纳秒UV激光加工配合振镜扫描的制孔方法可以提高盲孔的加工精度，并且加工孔径不受限制[10-11]。近年来，超短脉冲激光常被用于FR4覆铜板的盲孔加工。与纳秒UV激光相比，超短脉冲激光更高的峰值功率密度和更短的作用时间进一步降低了热效应并提高了加工精度[12-14]。

侧壁锥度是评价FR4覆铜板盲孔质量的关键指标，一方面为了确保层间连接的可靠性，应尽可能多地暴露盲孔底部的焊盘，另一方面，具有平滑侧壁且均匀倾斜的盲孔更利于后续的金属化流程，提高成品率。鉴于上述要求，盲孔底部直径与顶部直径之比须控制在70%～90%范围内[12,14-15]。现有研究缺乏对盲孔侧壁锥度进行有效调控的方案。另外，现有研究主要集中在浅盲孔，孔深超过500 μm的深盲孔制造仍面临较大挑战。五轴激光扫描技术是一项新兴的激光微加工技术，在控制扫描激光焦点三维坐标的同时，还可以对激光束的传输方向进行调控。当孔深增加时，倾斜传输的激光束可以避免被材料的表面和侧壁遮挡。该技术是调节深孔侧壁锥度和提升加工质量的有效方法[16-18]。

本文使用五轴激光扫描技术在厚度为960 μm的FR4覆铜板上实现了盲孔侧壁锥度的连续调控。盲孔的深径比可达4.9∶1，孔侧壁平直且粗糙度(S_a)小于5 μm。孔底没有残留玻璃纤维复合材料，底部铜层的损伤深度小于1 μm。研究结果表明，五轴激光扫描技术是提升FR4覆铜板盲孔加工精度和质量的有效手段。

2 实验装置及方法

图1展示了五轴飞秒激光钻孔装置、实验材料和加工方法。实验所用的光源为飞秒激光器，中心波长为1030 nm，脉冲宽度为436 fs。利用四分之一波片将扩束后的线偏振高斯光束转换为圆偏振，再利用自主开发的五轴扫描系统执行激光扫描[19]。其中，“五轴”指的是激光焦点在空间内的三轴坐标X、Y、Z，以及聚焦激光束在XOZ平面和YOZ平面上与Z轴的两个夹角α和β。XYZ三维位移工作台用于辅助实验样品的定位，定位完成后位移台不再运动。实验材料为FR4覆铜板，其中玻璃纤维复合材料(GFRP)层厚为925 μm，铜(Cu)层厚为35 μm。

盲孔的加工采用材料逐层去除法，加工开始时，激光焦点位于材料表面。每一层的激光扫描分为两个步骤。步骤1)：利用五轴扫描系统控制激光执行$XY\alpha\beta$

收稿日期：2023-04-25；**修回日期**：2023-05-25；**录用日期**：2023-05-29；**网络首发日期**：2023-07-04

基金项目：国家自然科学基金(52175405)

通信作者：*dlm@hust.edu.cn

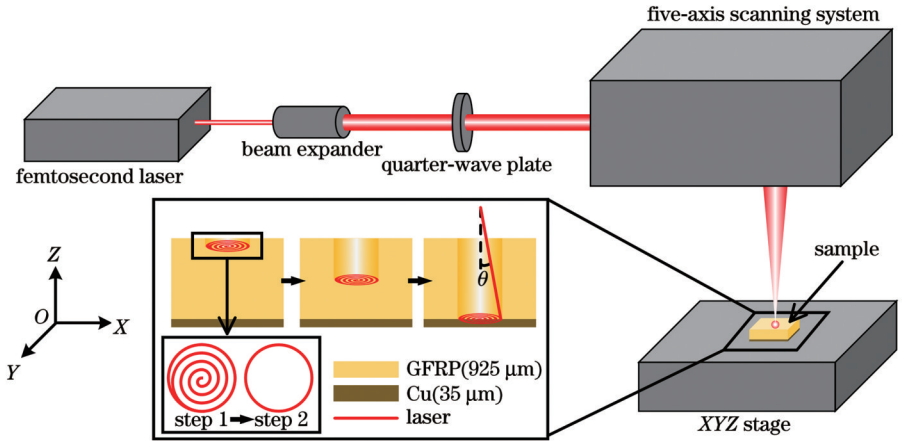

图 1　五轴飞秒激光钻孔实验装置、实验材料及加工方法

Fig. 1　Experimental setup of five-axis femtosecond laser drilling, experimental materials, and drilling strategy

四轴联合运动，使激光焦点在材料表面上绘制螺旋线，同时实时调节激光束的倾角（即图 1 中的角 θ，由 α 和 β 共同合成），避免孔侧壁对激光能量的遮挡。螺旋线的线间距为 l，代表螺旋线中相邻线条的间隔。然而，由于孔边缘处的激光搭接率低于孔内部，并且激光对倾斜侧壁的加工效率低于孔底部，侧壁处的材料去除进度将落后于孔底。步骤 2）：激光再绕着孔周扫描 n 次，增大侧壁处的材料去除速度。一层扫描结束后，五轴扫描系统控制激光焦点沿 Z 轴运动，使激光焦点再次落在材料表面上，去除下一层材料，直至盲孔加工完成。根据激光参数调节步骤 2）中的扫描次数 n 以及激光焦点每次运动的深度。加工时，使用与激光光轴同轴的压缩空气喷嘴，气压设置为 1 bar（1 bar=10^5 Pa）。加工完成后，采用激光共聚焦显微镜观察加工结果。具体的实验参数如表 1 所示。

表 1　实验参数

Table 1　Experimental parameters

Parameter	Value
Laser energy E /μJ	40, 70, 100
Laser repetition rate f /kHz	10, 25, 40
Laser scanning speed v /(mm·s^{-1})	100, 200, 300
Line spacing l /μm	7, 9, 11, 13, 15, 17

3　分析与讨论

3.1　激光参数对侧壁锥度的影响

为实现盲孔侧壁锥度的调节，首先研究了激光加工参数对侧壁锥度的影响，实验结果如图 2 所示。纳入研究的激光参数包括激光脉冲能量 E、重复频率 f 以及扫描速度 v。实验中采用的激光入射角度为 −6°，螺旋线的线间距 l 为 15 μm，扫描路径最外圈半径为 350 μm。加工完成后采用机械打磨的方式打磨出孔侧壁剖面并测量其侧壁锥度。图 2（a）展示的是不同加工参数下激光对孔边缘的修整总次数（n）与孔侧壁锥度的关系，其中激光脉冲能量设定为 40、70、100 μJ，重复频率设定为 10、25、40 kHz，扫描速度设定为 100、200、300 mm/s。采用最小二乘法将每组实验的散点数据点拟合为直线，直线的斜率代表该参数下激光对边缘修整的效率。图 2（b）～（d）展示了各加工参数对效率的影响规律，当脉冲能量由 40 μJ 上升至 100 μJ 时，直线的斜率由 -3.6×10^{-3} 下降到 -10.6×10^{-3}，远大于由重复频率和扫描速度变化引起的斜率变化，可见激光脉冲能量对孔侧壁锥度有重要的影响。因此，调节激光单脉冲能量是提升盲孔侧壁锥度加工效率的最有效手段。

3.2　填充间距对盲孔底部材料去除均匀度的影响

保证制孔过程中底部材料去除均匀性有助于减小激光对盲孔底部铜层的损伤，是实现深盲孔高精度加工的关键。影响孔底材料去除均匀性的主要因素是螺旋线的线间距 l，图 3 展示了线间距 l 对孔底材料去除的影响。实验选用的激光加工参数为激光脉冲能量 70 μJ、重复频率 25 kHz 和扫描速度 200 mm/s，每扫描完一层，激光焦点下降 20 μm，总扫描次数为 40 次，每层扫描结束后，激光沿孔周额外扫描 7 次以对孔壁进行修整。加工完成后使用激光共聚焦显微镜扫描盲孔的三维形貌。

当线间距 l 为 7 μm 时，微孔中间的加工效率高于边缘，中间部分的加工深度接近 925 μm，底部起伏较少，GFRP 层几乎被完全去除，而边缘部分的加工深度为 800 μm 左右，如图 3（a）所示。当线间距 l 增大到 9 μm 时，微孔中间的加工效率仍高于边缘，边缘部分的加工深度仍为 800 μm 左右，但微孔中间部分的加工效率有所下降，孔底向下凹陷，孔中心区域的加工深度接近 925 μm，其余部分的加工深度介于 800 μm 和 925 μm 之间，如图 3（b）所示。当线间距 l 增大到 11 μm 时，微孔中间的加工效率与边缘趋于一致，整个底部较为平整，加工深度均为 800 μm 左右，如图 3（c）所示。当线间距 l 增大到 13 μm 时，微孔中间部分的加工效率

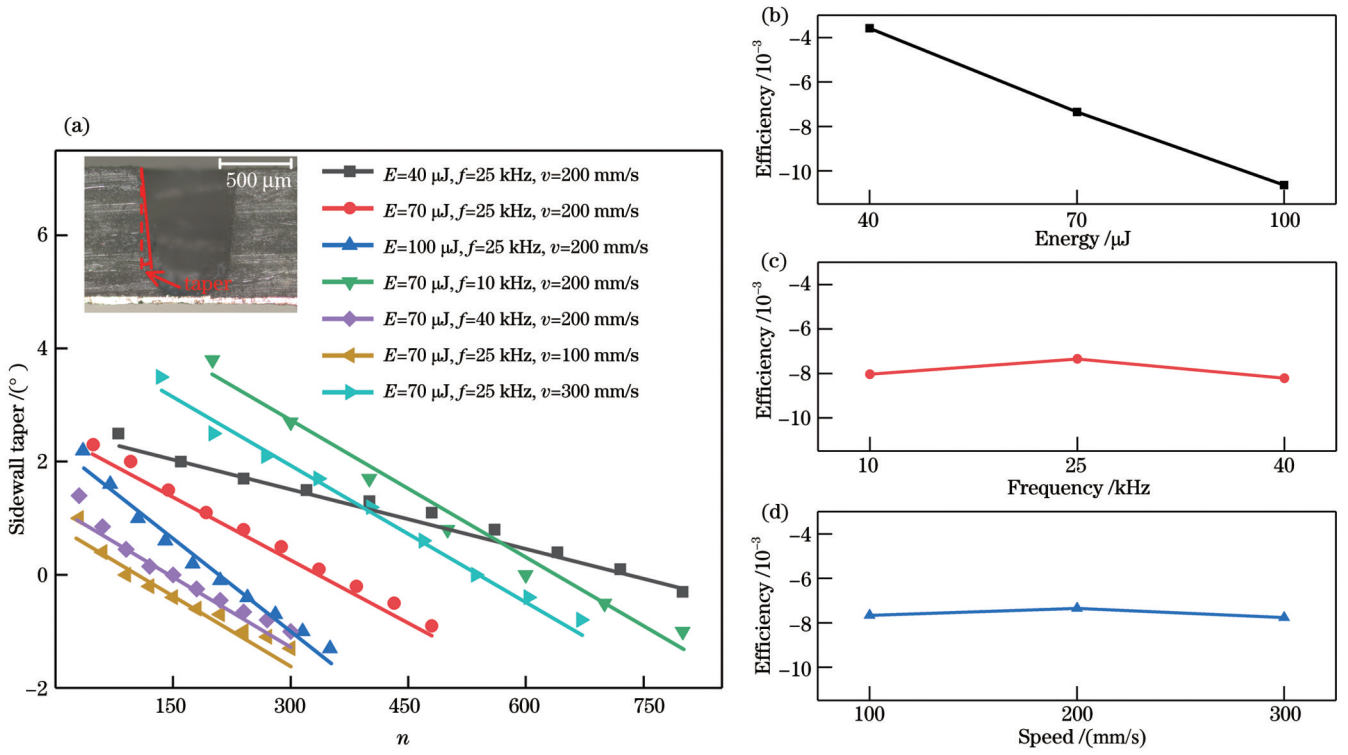

图 2 激光参数对侧壁锥度的影响。(a)不同激光参数下侧壁锥度随边缘修整总次数的变化;(b)不同激光能量下激光对边缘修整的效率;(c)不同激光频率下激光对边缘修整的效率;(d)不同激光扫描速度下激光对边缘修整的效率

Fig. 2 Influence of laser parameters on sidewall taper. (a) Sidewall taper versus n under different laser parameters; (b) efficiency of edge trimming by laser under different laser energy values; (c) efficiency of edge trimming by laser under different laser frequencies; (d) efficiency of edge trimming by laser under different laser scanning speeds

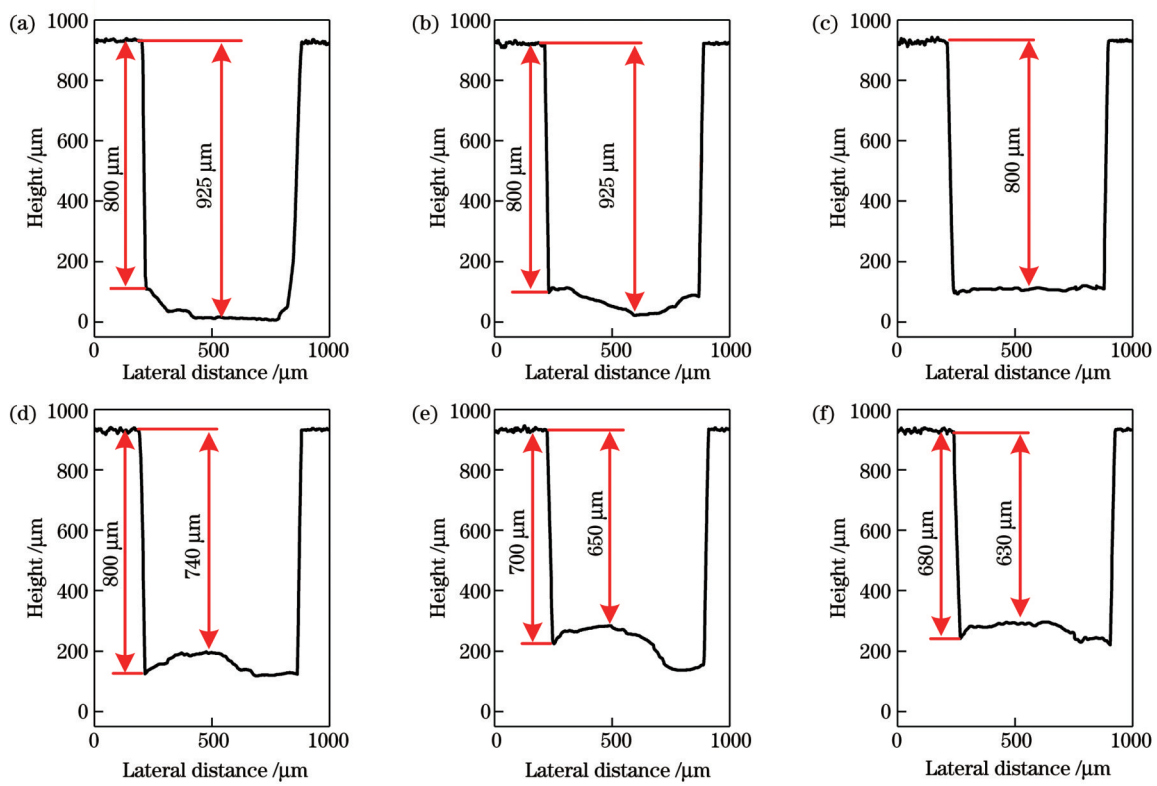

图 3 螺旋线的线间距对微孔底部材料去除均匀度的影响。(a)7 μm;(b)9 μm;(c)11 μm;(d)13 μm;(e)15 μm;(f)17 μm

Fig. 3 Influence of line spacing of spiral lines on material removal uniformity at micro-hole bottom. (a) 7 μm; (b) 9 μm; (c) 11 μm; (d) 13 μm; (e) 15 μm; (f) 17 μm

低于边缘区域，中间部分的材料向上突出，深度约为740 μm，边缘区域的加工深度仍为800 μm，如图3(d)所示。当线间距l增大到15 μm和17 μm时，中间部分的加工效率进一步降低，加工深度分别为650 μm和635 μm，同时，边缘部分的加工效率也受到影响，加工深度分别为700 μm和680 μm，如图3(e)、(f)所示。由上述分析可见，当线间距l较大或较小时，底部材料的去除不均匀现象较为明显，导致孔底材料的非对称分布，这个现象也与玻璃纤维材料的各向异性有关[20-21]。当填充间距与激光加工参数匹配时，材料的均匀去除得到保证，材料各向异性对材料去除均匀度的影响减弱。

3.3 盲孔侧壁锥度及孔径的调节

侧壁锥度调控的扫描策略如图4所示，其中R_{max}和R_{min}分别表示最大和最小半径。根据待加工盲孔的侧壁锥度，激光每扫描一层后螺旋线的最大半径减小，每层的半径减小量相同。每次扫描后边缘修整次数为3次。实验结果表明，当最小半径为231 μm时，孔壁锥度为6.0°，此时盲孔底部与入口的直径比为71.4%；随着R_{min}的逐渐上升，孔壁锥度逐渐下降，当R_{min}为293 μm时，孔壁锥度为2.5°，此时盲孔底部与入口的直径比为87.9%。实验测得的孔壁锥度略小于理论锥度，这代表每层加工时的边缘修整量略超出预期。进一步通过调节边缘修整次数或激光脉冲能量以及填充间距等加工参数，降低边缘修整量，实验值可以更贴近理论值。上述研究结果表明，本文提出的加工策略实现了盲孔锥度的连续可调，所得结果满足盲孔底部与入口的直径比在70%～90%区间的要求。同时，本加工技术还可以调节盲孔孔径，如图5所示。孔半径由350 μm逐渐下降到94 μm，盲孔的最大深径比达4.9∶1。半径为350 μm的盲孔的总加工时间为12.3 s，随着孔径的减小，需要去除的材料逐渐减少，需要的加工时间也逐渐减少。半径为190、138、94 μm的盲孔的加工总时间分别为8.3、7.0、5.7 s。

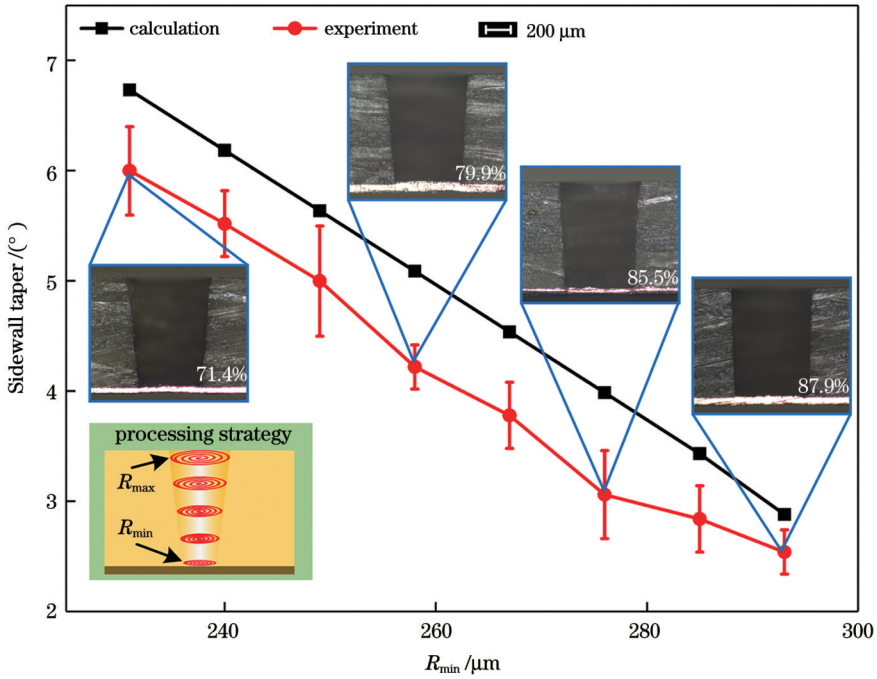

图4 侧壁锥度调节加工策略与实验结果

Fig. 4 Processing strategy and experimental results for sidewall taper regulation

3.4 盲孔底部加工质量的检测

盲孔底部的玻璃纤维复合材料残留情况以及铜层的损伤情况是评价盲孔加工质量的重要参数，图6展示了入口半径为350 μm、侧壁锥度为6.0°的盲孔的底部的检测结果。由于铜层较薄，在打磨过程中非常容易卷边，从而影响观察。因此，使用激光加工系统对盲孔进行半边切割，再使用激光共聚焦显微镜观察其形貌。孔侧壁平直，粗糙度S_a小于5 μm，如图6(a)所示；盲孔底部的玻璃纤维复合材料被完全去除，孔底部粗糙度S_a小于2 μm且圆度较好，如图6(b)所示；盲孔底部的铜层损伤深度小于1 μm，如图6(c)所示。

4 结 论

使用五轴激光扫描系统研究了FR4覆铜板深盲孔的飞秒激光加工技术，实现了FR4覆铜板深盲孔的高精度制造以及侧壁锥度的连续调控，提高了盲孔的加工质量。研究结果表明，相较于激光重复频率和扫描速度，激光脉冲能量对盲孔侧壁锥度的影响最为显著；调节扫描图形的线间距，使其与激光加工参数匹配，可以提高孔内材料的去除均匀性；通过改变激光扫描策略可以调节盲孔侧壁锥度，进而实现盲孔底部与

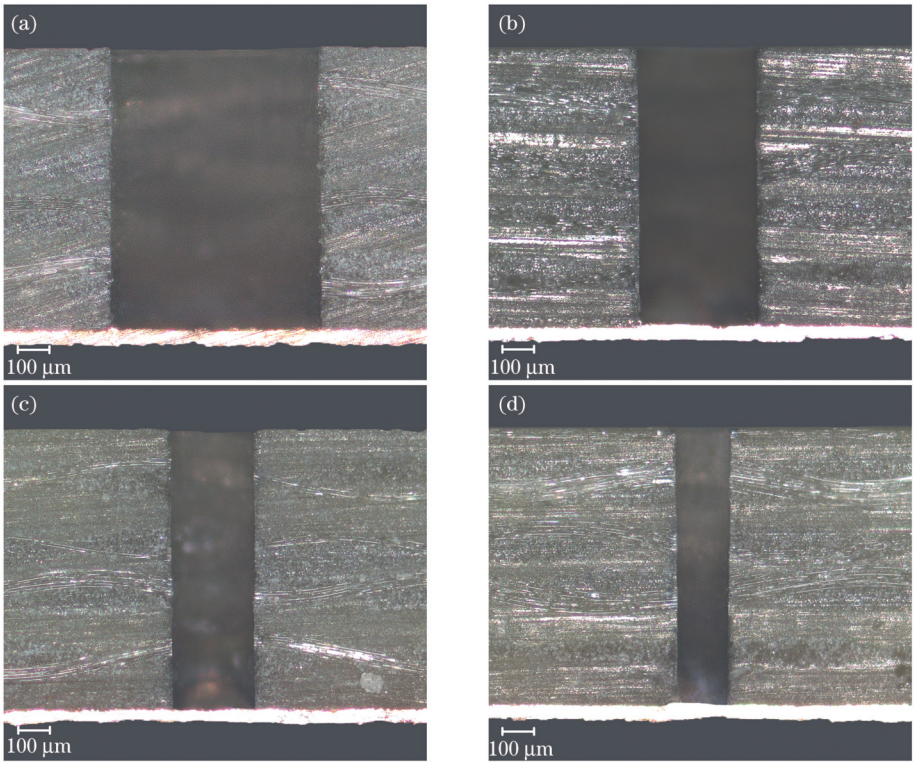

图 5　盲孔尺寸调节实验结果。(a)半径 350 μm;(b)半径 190 μm;(c)半径 138 μm;(d)半径 94 μm

Fig. 5　Experimental results of regulation of blind hole size. (a) Radius of 350 μm; (b) radius of 190 μm; (c) radius of 138 μm; (d) radius of 94 μm

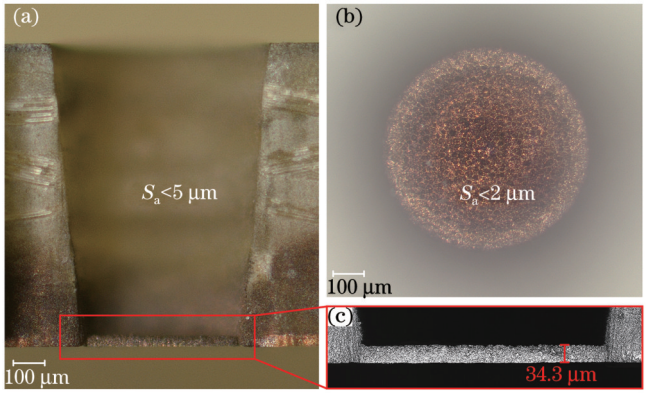

图 6　盲孔底部加工质量的检测。(a)侧壁形貌;(b)底部形貌;(c)铜层剖面形貌

Fig. 6　Detection of machining quality at blind hole bottom. (a) Morphology of sidewall; (b) morphology of bottom; (c) profile morphology of copper layer

入口的直径比在 70%～90% 区间的连续可调,同时也可以调节盲孔半径,最大的深径比可达 4.9∶1。盲孔底部加工结果表明,孔底的玻璃纤维复合材料被完全去除,底部铜层的损伤深度小于 1 μm。研究结果促进了五轴激光扫描技术的应用与发展。

参　考　文　献

[1] Liang X, Li B S, Fu L Y, et al. Mechanical drilling of PCB micro hole and its application in micro ultrasonic powder molding[J]. Circuit World, 2015, 41: 87-94.

[2] Cauwe M, Vandevelde B, Nawghane C, et al. High-density interconnect technology assessment of printed circuit boards for space applications[J]. Journal of Microelectronics and Electronic Packaging, 2020, 17(3): 79-88.

[3] Hasan M, Zhao J W, Jiang Z Y. A review of modern advancements in micro drilling techniques[J]. Journal of Manufacturing Processes, 2017, 29: 343-375.

[4] Owen M, Roelants E, Van Puymbroeck J. Laser drilling of blind holes in FR4/glass[J]. Circuit World, 1998, 24(1): 45-49.

[5] Kestenbaum A, D'Amico J F, Blumenstock B J, et al. Laser drilling of microvias in epoxy-glass printed circuit boards[J]. IEEE Transactions on Components, Hybrids, and Manufacturing Technology, 1990, 13(4): 1055-1062.

[6] Fang X Y, Yung K C. Copper direct drilling with tea CO_2 laser in manufacture of high-density interconnection printed circuit board [J]. IEEE Transactions on Electronics Packaging Manufacturing, 2006, 29(3): 145-149.[LinkOut]

[7] Zhou G Y, Li W B, Xiang Q Y, et al. Copper induced direct CO_2 laser drilling blind hole with the aid of brown oxidation for PCB CCL[J]. Applied Surface Science, 2019, 479: 512-518.

[8] Moorhouse C J, Villarreal F J, Baker H J, et al. Laser drilling of copper foils for electronics applications[J]. IEEE Transactions on Components and Packaging Technologies, 2007, 30(2): 254-263.

[9] Watson M N. Laser drilling of printed circuit boards[J]. Circuit World, 1984, 11(1): 13-29.

[10] Dunsky C. High-speed microvia formation with UV solid-state lasers[J]. Proceedings of the IEEE, 2002, 90(10): 1670-1680.

[11] Kim K R, Cho J H, Lee N Y, et al. High-precision and ultrafast UV laser system for next-generation flexible PCB drilling[J]. Journal of Manufacturing Systems, 2016, 38: 107-113.

[12] Franz D, Häfner T, Kunz T, et al. Ultrashort pulsed laser drilling of printed circuit board materials[J]. Materials, 2022, 15(11): 3932.

[13] Liu F H, Zhang R, Khurana G, et al. Smaller microvias for packaging interconnects by picosecond UV laser with a nanometer metal barrier layer: a feasibility study[J]. IEEE Transactions on Components, Packaging and Manufacturing Technology, 2020, 10

(8): 1411-1418.
[14] Lee D. Picosecond IR pulsed laser drilling of copper-coated glass/epoxy composite[J]. IEEE Transactions on Components, Packaging and Manufacturing Technology, 2017, 7(12): 2066-2072.
[15] Lei W S, Davignon J. Solid state UV laser technology for electronic packaging applications[J]. Proceedings of SPIE, 2005, 5629: 314-326.
[16] Romoli L, Vallini R. Experimental study on the development of a micro-drilling cycle using ultrashort laser pulses[J]. Optics and Lasers in Engineering, 2016, 78: 121-131.
[17] Mincuzzi G, Faucon M, Kling R. Novel approaches in zero taper, fast drilling of thick metallic parts by ultra-short pulse laser[J]. Optics and Lasers in Engineering, 2019, 118: 52-57.
[18] Zhu Q C, Fan P X, Li N, et al. Femtosecond-laser sharp shaping of millimeter-scale geometries with vertical sidewalls[J]. International Journal of Extreme Manufacturing, 2021, 3(4): 045001.
[19] Qiao Y Q, Yang H Z, Ding Y H, et al. Large scanning field laser concurrent drilling system with a five-axis independent control for special-shaped holes[J]. Optics Express, 2022, 31(1): 572-584.
[20] Hejjaji A, Singh D, Kubher S, et al. Machining damage in FRPs: laser versus conventional drilling[J]. Composites Part A: Applied Science and Manufacturing, 2016, 82: 42-52.
[21] Bhaskar V, Kumar D, Singh K K. Laser processing of glass fiber reinforced composite material: a review[J]. Australian Journal of Mechanical Engineering, 2019, 17(2): 95-108.

Femtosecond Laser Five-Axis Scanning Drilling of Deep Blind Holes

Qiao Yaqing[1], Tang Aiguo[1], Chen Tianting[1], Ma Haoran[1], Liu Yi[1], Gao Hui[1,2], Xiong Wei[1,2], Deng Leimin[1,2*]

[1]*Wuhan National Laboratory of Optoelectronics, Huazhong University of Science and Technology, Wuhan* 430074, *Hubei, China*;

[2]*Optical Valley Laboratory, Wuhan* 430074, *Hubei, China*

Abstract

Objective Processing blind holes in FR4 copper-clad boards to interconnect electronic components is an essential method in printing circuit boards. The quality of blind hole manufacturing is a crucial factor in determining device performance. Laser processing offers advantages such as high precision, no mechanical force, and flexible control, making it the primary method for machining blind holes in FR4 copper-clad boards. Recently, the application of ultrashort pulse lasers has reduced the thermal effects and improved drilling accuracy. However, current laser processing techniques still face challenges in controlling the taper of hole sidewalls and achieving sufficient hole depth. Sidewall taper is a crucial indicator for evaluating blind holes. To ensure reliable interlayer connections, the solder pad at the bottom of the blind hole should be exposed as much as possible. On the other hand, blind holes with uniformly inclined and smooth sidewalls are more conducive to subsequent metallization processes, thus improving the yield of finished products. Considering these conflicting requirements, the ratio of the bottom diameter to the top diameter of blind holes must be controlled within the range of 70%-90%. Furthermore, existing research primarily focuses on shallow blind holes, and the manufacturing of deep blind holes with depths exceeding 500 μm still presents significant challenges. In this study, we adopt five-axis laser scanning technology to avoid obstruction of the laser beam by the material surface and sidewalls in order to achieve sidewall taper adjustment and improve blind hole depth.

Methods In this study, a five-axis laser scanning system with a wavelength of 1030 nm and a pulse width of 436 fs is employed to perform laser scanning. The experimental material is an FR4 copper-clad board, with the glass fiber composite material thickness of 925 μm and the copper thickness of 35 μm. The processing of blind holes adopts a layer-by-layer material removal method. The processing of each layer is divided into two steps. In step 1, the laser draws a spiral line on the material surface, and in step 2, the laser performs additional scanning around the hole circumference to increase the material removal rate at the sidewalls. Simultaneously, during the laser scanning of the two-dimensional pattern, the five-axis scanning system controls the tilt angle of the laser beam to avoid obstruction of laser energy by the hole sidewalls. After the scanning is completed for one layer, the laser focus moves downward to process the next layer of material until the blind hole processing is finished. Compressed air at a pressure of 1 bar (1 bar=10^5 Pa) is supplied coaxially. The processed results are observed using a laser confocal microscope.

Results and Discussions Compared to laser repetition rate and scanning speed, the impact of laser pulse energy on the sidewall taper is more significant (Fig. 2). Modifying the line spacing of the spiral pattern can enhance the uniformity of material removal at the bottom of the hole and mitigate the influence of material anisotropy on the uniformity of material removal (Fig. 3). By adjusting the scanning strategy, continuous control over the sidewall taper and hole geometry dimensions can be achieved (Figs. 4 and 5). The hole sidewalls are straight with surface roughness (S_a) of less than 5 μm. The glass fiber composite material at the bottom of the blind hole is thoroughly removed, with a bottom roughness of less than 2 μm and good roundness. The damage depth to the copper layer at the bottom of the blind hole is less than 1 μm (Fig. 6).

Conclusions This study investigates the femtosecond laser machining technology for deep blind holes in FR4 copper-clad boards using a five-axis laser scanning system. The research demonstrates that, compared with laser repetition rate and scanning speed, the variation in laser pulse energy has the most significant impact on the sidewall taper of blind holes. Matching the line spacing of the

scanning pattern with laser processing parameters can improve the uniformity of material removal inside the holes. By adjusting the laser scanning strategy, the sidewall taper of blind holes can be controlled, allowing for continuous and adjustable diameter ratios between the bottom and entrance of the blind hole within the range of 70%-90%. It also enables the adjustment of the blind hole radius, with a maximum aspect ratio of 4.9∶1. Inspection of the drilling results at the bottom of the blind hole reveals complete removal of the glass fiber composite material, with a copper layer damage depth below 1 μm. This research achieves high-precision manufacturing of deep blind holes in FR4 copper-clad boards and continuous control of sidewall taper, enhancing the quality of blind hole machining and promoting the application and development of five-axis laser scanning technology.

Key words laser technique; laser drilling blind hole; five-axis laser scanning; sidewall taper; femtosecond laser